

# Discovery of a Young L Dwarf Binary, SDSS J224953.47+004404.6AB<sup>1</sup>

K. N. Allers<sup>2,3</sup>

*Department of Physics and Astronomy, Bucknell University, Lewisburg, PA 17837, USA;  
k.allers@bucknell.edu*

Michael C. Liu<sup>4</sup>, Trent J. Dupuy, Michael C. Cushing<sup>3</sup>

*Institute for Astronomy, University of Hawaii, 2680 Woodlawn Drive, Honolulu, HI 96822,  
USA*

## ABSTRACT

We report discovery of a young 0'32 L dwarf binary, SDSS J2249+0044AB, found as the result of a Keck laser guide star adaptive optics imaging survey of young field brown dwarfs. Weak K I, Na I, and FeH features as well as strong VO absorption in the integrated-light *J*-band spectrum indicate a low surface gravity and hence young age for the system. From spatially resolved *K*-band spectra we determine spectral types of  $L3 \pm 0.5$  and  $L5 \pm 1$  for components A and B, respectively. SDSS J2249+0044A is spectrally very similar to G196-3B, an L3 companion to a young M2.5 field dwarf. Thus, we adopt 100 Myr (the age estimate of the G196-3 system) as the age of SDSS J2249+0044AB, but ages of 12–790 Myr are possible. By comparing our photometry to the absolute magnitudes of G196-3B, we estimate a distance to SDSS J2249+0044AB of  $54 \pm 16$  pc and infer a projected separation of  $17 \pm 5$  AU for the binary. Comparison of the luminosities to evolutionary models at an age of 100 Myr yields masses of  $0.029 \pm 0.006$  and  $0.022^{+0.006}_{-0.009} M_{\odot}$  for SDSS J2249+0044A and B, respectively. Over the possible ages of the system (12–790 Myr), the mass of SDSS J2249+0044A could range from 0.011 to 0.070  $M_{\odot}$  and the mass of SDSS J2249+0044B could range from 0.009 to 0.065  $M_{\odot}$ . Evolutionary models

---

<sup>2</sup>Institute for Astronomy, University of Hawaii, 2680 Woodlawn Drive, Honolulu, HI 96822

<sup>3</sup>Visiting Astronomer at the Infrared Telescope Facility, which is operated by the University of Hawaii under Cooperative Agreement no. NCC 5-538 with the National Aeronautics and Space Administration, Office of Space Science, Planetary Astronomy Program.

<sup>4</sup>Alfred P. Sloan Research Fellow

predict that either component could be burning deuterium, which could result in a mass ratio as low as 0.4, or alternatively, a reversal in the luminosities of the binary. We find a likely proper motion companion, GSC 00568-01752, which lies  $48''.9$  away (a projected separation of 2600 AU) and has Sloan Digital Sky Survey and Two Micron All Sky Survey colors consistent with an early M dwarf. We calculate a photometric distance to GSC 00568-01752 of  $53 \pm 15$  pc, in good agreement with our distance estimate for SDSS J2249+0044AB. The space motion of SDSS J2249+0044AB shows no obvious coincidence with known young moving groups, though radial velocity and parallax measurements are necessary to refine our analysis. The unusually red near-IR colors, young age, and low masses of the binary make it an important template for studying planetary-mass objects found by direct imaging surveys.

*Subject headings:* binaries: visual, infrared: stars, stars:low-mass

## 1. Introduction

Brown dwarfs are objects with masses too low to sustain hydrogen burning in their cores. Because they continually cool over their lifetimes, substellar objects are much more luminous when they are young. For example, a  $0.02 M_{\odot}$  brown dwarf at 10 Myr is  $\sim 5000$  times more luminous than it will be at 3 Gyr, roughly the age of the general field population (Burrows et al. 2001). Similarly, planetary-mass objects ( $M \lesssim 0.012 M_{\odot}$ ) are expected to be more luminous when young. In fact, the first directly imaged planets outside of our solar system were detected as companions to young host stars (Kalas et al. 2008; Marois et al. 2008). Unfortunately, the fundamental properties (masses and temperatures) of these planets are difficult to determine because their bright host stars inhibit a detailed spectroscopic study. Photometry of the planets can be compared to evolutionary models (Baraffe et al. 2003; Fortney et al. 2008) to infer masses and temperatures, but such models remain untested in the planetary-mass regime.

Young brown dwarfs provide a unique opportunity for direct study of planetary-mass companions. Extremely low-mass objects ( $\lesssim 1 M_{Jupiter}$ ) are within the reach of direct detection because such objects are self-luminous at young ages. A brown dwarf primary is

---

<sup>1</sup>Some of the data presented herein were obtained at the W.M. Keck Observatory, which is operated as a scientific partnership among the California Institute of Technology, the University of California and the National Aeronautics and Space Administration. The Observatory was made possible by the generous financial support of the W.M. Keck Foundation.

itself faint, which means the properties of the planetary-mass companion are not masked by a bright parent star. To date, 2MASSW J1207334-393254 (hereafter 2MASS 1207) is the only known young brown dwarf having a planetary-mass companion, 2MASS 1207b (Chauvin et al. 2005; Song et al. 2006). 2MASS 1207b has proven to be quite interesting, as it is under-luminous for its temperature and age compared to evolutionary models (Mohanty et al. 2007; Biller & Close 2007). It is unclear if 2MASS 1207b formed in an unusual way (Mamajek & Meyer 2007), is occulted by a circumstellar disk (Mohanty et al. 2007), or if the problem lies in the evolutionary models themselves. Finding and characterizing additional planetary companions to young brown dwarfs can provide critical tests for evolutionary models as well as empirical templates for comparison to other young planets.

Most of the known young brown dwarfs are members of star-forming regions (e.g., Muench et al. 2007; Lucas et al. 2006; Allers et al. 2006) which renders them unsatisfactory for imaging surveys searching for planetary-mass companions for a number of reasons. First, brown dwarfs in star-forming regions are often attenuated by natal cloud material, which can inhibit the determination of the object’s fundamental properties. Second, even the nearest star-forming regions are quite distant ( $\sim 125$  pc) making the planetary-mass objects faint. Lastly, current imaging surveys can reach angular resolutions of  $\sim 80$  mas, which at a distance of 125 pc corresponds to  $\sim 10$  AU. Field dwarf binaries tend to have small (3–10 AU) separations (Burgasser et al. 2007), which means if companions to young brown dwarfs have similar separations, they would remain unresolved.

To search for planetary-mass companions at small separations we are carrying out a Keck laser guide star adaptive optics (LGS AO) survey to image young ( $\lesssim 100$  Myr), nearby ( $\lesssim 80$  pc) brown dwarfs. This paper presents the early results of our survey (see also Allers et al. 2009) which is part of a larger, ongoing effort using LGS AO to study the multiplicity of brown dwarfs and determine their properties (e.g., Liu & Leggett 2005; Liu et al. 2006; Dupuy et al. 2009; Liu et al. 2010).

Using Keck LGS AO, we have discovered a new young binary system, SDSS J224953.47+004404.6AB (hereinafter SDSS J2249+0044AB). SDSS J2249+0044AB was first identified by Geballe et al. (2002) as an L5 dwarf based on near-IR spectroscopy. Hawley et al. (2002) obtained optical spectroscopy of SDSS J2249+0044AB and assigned it a spectral type of L3. The discrepant near-IR and optical spectral types and the unusually red near-IR colors ( $J - K = 2.05$  mags) of SDSS J2249+0044AB were emphasized by Leggett et al. (2002) and Knapp et al. (2004). Nakajima, Tsuji, & Yanagisawa (2004) were the first work to point out the spectral peculiarities of SDSS J2249+0044AB, namely weak K I absorption lines in its  $J$ -band spectrum and the prominent triangular shape of its  $H$ -band spectrum. Other work (e.g., Lucas et al. 2001; Gorlova et al. 2003) attributes these spectral peculiarities to a low-gravity (young)

atmosphere.

In this paper, we present multi-wavelength imaging and spectroscopy used to determine the properties of SDSS J2249+0044AB.

## 2. Observations

### 2.1. Keck LGS AO/NIRC2 Imaging

We imaged SDSS J2249+0044AB on 2006 October 13 and 2008 September 8 (UT) using the facility IR camera, NIRC2, of the Keck II Telescope on Mauna Kea, Hawaii and the LGS AO system (Wizinowich et al. 2006; van Dam et al. 2006). We used the narrow field camera ( $10''.2 \times 10''.2$  field of view) and the Mauna Kea Observatories (MKO)  $J, H, K_S$ , and  $L'$  filters (Simons & Tokunaga 2002; Tokunaga, Simons & Vacca 2002). For the  $JHK_S$  filters, we used an exposure time of 60 s and obtained a series of six dithered images in each filter, offsetting the telescope by a few arcseconds. The images were reduced in the standard fashion (dome flat-fielded, median sky-subtracted, registered and stacked). The  $L'$ -band data were taken using a 10-point dither pattern with 200 coadds of 0.3 s integration per image. The  $L'$ -data were reduced in a similar manner as the  $JHK_S$  data, except that flat fields were constructed from the science frames themselves and sky subtraction was done in a pairwise fashion using consecutive frames.

To measure the flux ratios and relative positions of the binary’s two components, we used an analytic model of the point-spread function (PSF) as the sum of three elliptical Gaussians (Liu et al. 2006; Allers et al. 2009). We used the astrometric calibration from Ghez et al. (2008), with a pixel scale of  $9.963 \pm 0.005$  mas pixel<sup>-1</sup> and an orientation for the detector’s  $+y$ -axis of  $+0^\circ.13 \pm 0^\circ.02$  east of north. After applying the distortion correction developed by B. Cameron (2007, private communication), the resulting mean astrometry changed by less than  $1\sigma$ ; however, the rms errors were significantly improved. For example, in the  $K_S$  band data set the measured separation scatter was reduced from 0.7 to 0.2 mas and the position angle (P.A.) scatter from  $0^\circ.14$  to  $0^\circ.03$ . Table 1 summarizes the resulting astrometry and binary flux ratios, with uncertainties derived from the rms scatter of measurements for individual dithers. For objects at  $\gtrsim 0''.8$  separation, the final stacked mosaics reach  $10\sigma$  detection limits for point sources of  $\sim 21.8$ ,  $\sim 22.5$  and  $\sim 21.6$  mags at  $JHK_S$ , respectively. The separation and P.A. of the system show no significant change between our 2006 October 13 and 2008 September 8 (UT) observations. Given the proper motion of SDSS J2249+0044AB ( $\mu = 82.8 \pm 3.7$  mas yr<sup>-1</sup>, PA= $85^\circ.4 \pm 2^\circ.5$  Bramich et al. 2008), our two epochs of imaging indicate that the system is co-moving and physically associated.

In order to assess additional systematic errors in our NIRC2 measurements, we applied our PSF-fitting routine to simulated binary images. Only the  $K_S$  and  $L'$  data sets had appropriate PSF reference observations (single objects with similar Strehl and FWHM), and we found negligible (below  $1\sigma$ ) systematic offsets in these simulations. We also note that astrometry measured in multiple bandpasses in 2006 October is remarkably consistent: the  $\chi^2$  of the separation and P.A. measurements are 0.60 and 0.28, respectively, for an expected value of 1.37. Such good agreement implies that our astrometric errors are reasonable. We also found insignificant offsets ( $< 0.01$  mas,  $< 0''.006$ ) due to differential chromatic refraction (DCR) by using the resolved  $K_S$  band spectra of the two components and template  $J$  and  $H$  band spectra to derive offsets in the same manner as Dupuy et al. (2009). Finally, we accounted for the uncertainty in the astrometric calibration by adding these errors in quadrature to the separation and P.A. measurements.

## 2.2. IRTF/SpeX Near-IR Spectroscopy

Integrated-light near-IR spectroscopy of SDSS J2249+0044AB was obtained on 2006 November 19 (UT) using the SpeX spectrograph (Rayner et al. 2003) on the NASA Infrared Telescope Facility (hereinafter IRTF). A series of 18 exposures of 180 seconds each were taken, nodding along the slit, for a total integration time of 54 minutes. The seeing recorded by the IRTF was  $0''.5$ . The data were taken using the Low-Res prism with the  $0''.5$  slit aligned with the parallactic angle, producing a  $0.8$ – $2.5$   $\mu\text{m}$  spectrum with a resolution ( $R=\lambda/\Delta\lambda$ ) of  $\sim 150$ . For telluric correction of our SDSS J2249+0044AB spectrum, we observed a nearby A0V star, HD 216807 and obtained calibration frames (flats and arcs) in between sets of SDSS J2249+0044AB observations. We flux-calibrated our spectrum of SDSS J2249+0044AB using integrated-light  $JHK$  photometry from Knapp et al. (2004) and published Vega flux densities for the MKO filter system (Tokunaga & Vacca 2005). For comparison to our SDSS J2249+0044AB spectrum, we obtained SpeX spectra of 2MASS J05012406-0010452 (L4, hereinafter 2MASS 0501-0010; Cruz et al. 2009; Reid et al. 2008), 2MASS J22244381-0158521 (L4.5, hereinafter 2MASS 2224-0158; Kirkpatrick et al. 2000) and G196-3B (L3; Cruz et al. 2009) on 2008 September 24, 2008 November 30, and 2009 January 28 respectively. We used the same instrument setup as for our spectrum of SDSS J2249+0044AB and obtained total integration times of 20–28 minutes per source. The spectra were reduced using the facility reduction pipeline, Spextool (Cushing et al. 2004), which includes a correction for telluric absorption following the method described in Vacca et al. (2003). Our SpeX spectra are presented in Figures 2 and 3.

### 2.3. Keck LGS AO/OSIRIS Imaging and Spectroscopy

On 2008 September 9 (UT), we obtained imaging of SDSS J2249+0044AB using Keck LGS AO and the imaging camera of OSIRIS (Larkin et al. 2003). The field of view of the OSIRIS imager is  $20''.4 \times 20''.4$  with a plate scale of  $20 \text{ mas pixel}^{-1}$ . We obtained a series of seven dithered images using the *Zbb* ( $\lambda_{\text{center}}=1.0915 \mu\text{m}$ ,  $\Delta\lambda=0.2203 \mu\text{m}$ ) and the *Hn1* ( $\lambda_{\text{center}}=1.5037 \mu\text{m}$ ,  $\Delta\lambda=0.0747 \mu\text{m}$ ) filters with exposure times of 120 s and 180 s per image, respectively. The resulting images were dome-flatfielded, median sky-subtracted, registered and stacked.

We measured the flux ratios and astrometry of the binary using a similar technique as for our NIRC2 images (Section 2.1). For the OSIRIS imager, there is no astrometric calibration available, so we used the nominal pixel scale of  $0''.020 \text{ pixel}^{-1}$ . Comparing the OSIRIS astrometry from UT 2009 September 9 to the NIRC2 measurements from the previous night, we find a  $2.8\sigma$  difference in separation, implying a systematic error of 4% in the OSIRIS imager pixel scale. A pixel scale of  $0''.0208 \text{ pixel}^{-1}$  would bring the two data sets into agreement. There is no significant P.A. offset between the two data sets to within  $0^\circ.6$ . In the following analysis, we only require the flux ratios from the OSIRIS imaging, which is not affected by astrometric calibration of OSIRIS. A summary of the data is presented in Table 1, and the images are displayed in Figure 1. To flux calibrate our OSIRIS photometry, we compute synthetic integrated-light *Zbb* and *Hn1* flux densities from our SpeX spectrum of SDSS J2249+0044AB. Following the method of Tokunaga & Vacca (2005), we calculate Vega flux densities of  $4.87 \times 10^{-9}$  and  $1.55 \times 10^{-9} \text{ W m}^{-2} \mu\text{m}^{-1}$  for the *Zbb* and *Hn1* filters, respectively. We then convert the synthetic integrated-light *Zbb* and *Hn1* flux densities of SDSS J2249+0044AB into Vega-system magnitudes and use our measured flux ratios to calculate the magnitudes of each component (Table 2).

We obtained spatially resolved *K*-band spectroscopy of SDSS J2249+0044AB on 2008 August 23 (UT) using the facility near-IR integral field spectrograph, OSIRIS, and LGS AO on the Keck-II Telescope. We selected the 35 mas pixel scale for our observations. We observed SDSS J2249+0044AB using the *Kbb* spectrograph filter ( $1.96\text{--}2.38 \mu\text{m}$ ), taking six dithered exposures of 600 s each, for a total of 1 hr on source integration. The FWHM, as measured on the stacked two-dimensional (2D) images of SDSS J2249+0044AB, was 70 mas; thus the binary ( $\rho=322.8 \text{ mas}$ ) is well resolved. Immediately following our observations of SDSS J2249+0044AB, we obtained spectra of a nearby A0V star, HD 210501, in order to correct for telluric absorption. The initial reduction from 2D images to 3D data cubes was accomplished using the OSIRIS data reduction pipeline (Krabbbe et al. 2004). The individual spectra for each component were then extracted from the 3D data cubes by summing the flux in fixed apertures of  $175 \times 175 \text{ mas}$  at each wavelength. The resulting spectra

for each component were median-combined together, and uncertainties were determined from the standard deviation at each wavelength. Telluric correction and flux calibration were performed using the observations of the A0 V standard and the technique described in Vacca et al. (2003). The resulting 1.96–2.38  $\mu\text{m}$  spectra of SDSS J2249+0044A and B (Figure 4) have a resolution ( $\lambda/\Delta\lambda$ ) of  $\sim 3800$  and a median signal-to-noise ratio (S/N) per resolution element of  $\sim 55$  and  $\sim 30$  for SDSS J2249+0044A and B, respectively.

## 2.4. *Spitzer*/IRAC Imaging

We measured IRAC photometry for SDSS J2249+0044AB from observations taken as a part of *Spitzer* program 50059 (PI: A. Burgasser). Using the IDLPhot package,<sup>5</sup> we measured aperture photometry from mosaicked images created by the *Spitzer* Science Center (pipeline version 18.7.0). We calculated the flux in a  $3''.6$  aperture, using a background annulus of 12–24'', and applied the aperture corrections recommended by the IRAC Data Handbook. Table 2 lists our measured IRAC photometry for SDSS J2249+0044AB. The uncertainties in our measured photometry (including photometric and calibration uncertainties) were less than 0.02 mag, but we choose to adopt the more conservative 0.05 mag uncertainty recommended by the IRAC Data Handbook. As a check, we measured photometry for five young L3 and L4 dwarfs with published IRAC photometry (Luhman et al. 2009) and found that our photometry agreed to better than 0.02 mag with previously published results.

## 3. Analysis

### 3.1. Spectral Type

SDSS J2249+0044AB was originally assigned a composite near-IR spectral type of L5 $\pm$ 1 by Geballe et al. (2002) and an optical spectral type of L3 by Hawley et al. (2002). The spectral type sensitive index ( $\langle F_{\lambda=1.550-1.560} \rangle / \langle F_{\lambda=1.492-1.502} \rangle$ ) of Allers et al. (2007), which is calibrated for young and field stars with optical spectral types, suggests a spectral type of L4  $\pm$  1, in agreement with both the Geballe et al. (2002) and Hawley et al. (2002) spectral types.

We determine spectral types for each component from the spatially resolved OSIRIS *K*-band spectroscopy of SDSS J2249+0044A and B shown in Figure 4. For comparison we

---

<sup>5</sup><http://idlastro.gsfc.nasa.gov/>

also show spectra of a young L3 dwarf, G196-3B from Allers et al. (2007); an L4.5 type dwarf with a dusty photosphere, 2MASS 2224-0158 from Cushing et al. (2005); and “normal” field L3 and L5 dwarfs, 2MASS J15065441+1321060 and 2MASS J15074769-1627386 (hereinafter 2MASS 1506+1321 and 2MASS 1507-1627) from Cushing et al. (2005). The  $K$ -band spectra of young field dwarfs do not appear to differ significantly in shape or features from the spectra of field dwarfs. Qualitatively, the spectra of SDSS J2249+0044A and B are quite similar to the spectra of field L3 and L5 dwarfs respectively, and SDSS J2249+0044A appears to be of a similar spectral type to G196-3B (young L3, Cruz et al. 2009).

Another method of assigning spectral type is using spectral indices. Table 3 lists the index values and derived spectral types for SDSS J2249+0044A and B from  $K$ -band spectral indices available in the literature. These indices, however, are calibrated for field dwarfs, and their applicability to young objects has not been proven. We tested the indices in Table 3 on our spectrum of G196-3B, and found that each index reproduced its L3 optical spectral type to within one subtype. We also compared our  $K$ -band spectra of SDSS J2249+0044A and B to L dwarf spectra from Cushing et al. (2005) and determined the best fitting L dwarf spectrum via  $\chi^2$  minimization. The fits to the spectra of SDSS J2249+0044A and B show minima in  $\chi^2$  at spectral types of  $L3\pm 1$  and  $L6\pm 2$ , respectively.<sup>6</sup> From the weighted mean of the spectral types determined from  $\chi^2$  fitting and calculated from spectral indices (Table 3), we assign spectral types of  $L3\pm 0.5$  and  $L5\pm 1$  to SDSS J2249+0044A and B, respectively.<sup>7</sup>

### 3.2. Age

As noted by Leggett et al. (2002) and Knapp et al. (2004), SDSS J2249+0044AB has unusually red colors ( $J - K = 2.05$  mag) compared to the other L5 dwarfs in their samples ( $J - K$  of 1.41–1.88 mag). Resolved as a binary with spectral types of L3 and L5, the red near-IR colors of SDSS J2249+0044A and B become even more dramatic relative to field dwarfs of the same spectral type (Figure 5). There are currently two explanations for unusually red  $J - K$  colors of single L dwarfs: youth (Kirkpatrick et al. 2006) and/or a metal-rich (dusty) photosphere (Looper et al. 2008; Cushing et al. 2005). Interestingly, though the  $J - K$  colors of young and dusty L dwarfs are similar, the  $K - L'$  colors of SDSS J2249+0044A and B are significantly redder than the  $K - L'$  of the dusty L dwarf

---

<sup>6</sup>Uncertainties in the  $\chi^2$  fit are determined from the spectral types of Cushing et al. (2005) spectra where  $\chi^2 = \chi_{\min}^2 + 1$ .

<sup>7</sup>Uncertainties in the spectral types were determined from the weighted average variance of the results of  $\chi^2$  fitting combined with the values reported in Table 3.

2MASS 2224-0158 (Golimowski et al. 2004). This hints that young and dusty objects may be distinguished on the basis of their  $K-L'$  colors, though additional  $L'$  measurements are necessary to establish a set of robust color selection criteria.

Figure 3 shows the composite near-IR spectrum of SDSS J2249+0044AB compared to an L4.5 dwarf with a dusty photosphere (2MASS 2224-0158; Cushing et al. 2005), a low-gravity (young) L4 field dwarf (2MASS 0501-0010; Cruz et al. 2009), a young L3 field dwarf (G196-3B; Rebolo et al. 1998; Kirkpatrick et al. 2001; Cruz et al. 2009), and a “normal” field L3 (2MASS 1506+1321; Burgasser 2007). The spectrum of SDSS J2249+0044AB shows several hallmarks of low gravity. The FeH bands (particularly at 1.0 and 1.55  $\mu\text{m}$ ) in the spectrum of SDSS J2249+0044AB are weaker than seen in the dusty or normal field dwarfs. The VO band (1.05  $\mu\text{m}$ ) is stronger in SDSS J2249+0044AB than in the older field dwarfs. Though the Na I and K I features are blended with other features at this spectral resolution, they appear to be weaker in the spectrum of SDSS J2249+0044AB than in the older field objects. Nakajima, Tsuji, & Yanagisawa (2004) found that (at  $R \simeq 400$ ) the K I lines are weaker in their  $J$ -band spectrum of SDSS J2249+0044AB than in field dwarfs of similar spectral type. The spectrum of SDSS J2249+0044AB also shows the triangular  $H$ -band continuum shape characteristic of young objects (e.g., Lucas et al. 2001; Kirkpatrick et al. 2006).

Though the spectrum of SDSS J2249+0044AB shows hallmarks of low-gravity (youth), it is not possible to obtain a precise age for the system. SDSS J2249+0044AB does not have a measured parallax, so using evolutionary models to determine its age is not possible. There are also no known age fiducials for mid-L-type objects showing spectral signatures of youth. A strict upper limit on the age of SDSS J2249+0044AB can be determined from the youngest L dwarf showing *no* spectral signatures of youth. HD 130948BC, an L4+L4 binary, has a well established age of  $790^{+220}_{-150}$  Myr (Dupuy et al. 2009), and its near-IR spectra show no hallmarks of low-gravity (Goto et al. 2002; Potter et al. 2002).<sup>8</sup> Because SDSS J2249+0044AB is not spatially coincident with other known young objects, it has to be old enough that its natal cluster has dispersed. For a lower limit on the age, this means SDSS J2249+0044AB

---

<sup>8</sup>We note that our upper age limit is significantly older than that of Kirkpatrick et al. (2008), who suggest that spectral signatures of youth in low-resolution optical spectra should be readily discernable for objects Pleiades age and younger ( $\lesssim 100$  Myr). We note, however, that Kirkpatrick et al. (2008) detect subtle signatures of youth in the optical spectrum of G1417BC, an L4.5+L4.5 dwarf companion system to G1417A (a G0 dwarf). Using the method described in detail by Dupuy et al. (2009), we calculate an age for G1417A of  $750^{+140}_{-120}$  Myr from gyrochronology (Barnes 2007; Mamajek & Hillenbrand 2008). Thus, the  $\sim 100$  Myr upper age limit of Kirkpatrick et al. (2008) is possibly an underestimate, and L-type objects displaying spectral signatures of youth in the optical could be significantly older. We note that the near-IR spectrum of G1417BC (Reid et al. 2001a; Testi et al. 2001) does not show the same strong IR signatures of youth as SDSS J2249+0044AB, suggesting that SDSS J2249+0044AB is likely younger.

must be at least as old as the youngest known moving groups, the TW Hydra and  $\beta$  Pic associations ( $\sim 12$  Myr; Mentuch et al. 2008; Zuckerman et al. 2001).

We can also compare SDSS J2249+0044AB to G196-3B, an L3 companion to an M2.5 dwarf with an age of  $\sim 100$  Myr, but with possible ages spanning 20–300 Myr (Rebolo et al. 1998; Kirkpatrick et al. 2001; Shkolnik et al. 2009). Given the remarkable spectral similarity of SDSS J2249+0044AB and G196-3B, we adopt an age of  $\sim 100$  Myr for SDSS J2249+0044AB, but acknowledge that this age is highly uncertain and could range from 20–300 Myr (the age range of G196-3B). Ages as young as 12 Myr and as old as 790 Myr, though unlikely, can not be completely ruled out and are the strict upper and lower limits on the age of SDSS J2249+0044AB. The large uncertainties associated with determining the age of SDSS J2249+0044AB highlight the need for observations of benchmark low-gravity L dwarfs with well determined ages.

### 3.3. Bolometric Magnitudes

To calculate the bolometric flux of SDSS J2249+0044AB, we combined our flux calibrated SpeX spectrum with available photometry (Table 2) to create a 0.75–7.87  $\mu\text{m}$  spectral energy distribution (SED). For wavelengths greater than 7.87  $\mu\text{m}$ , we assume a Rayleigh-Jeans spectrum. We also extended our SED to shorter wavelengths assuming a linear SED from the flux at  $i$  band to zero flux at zero wavelength. Using a Monte Carlo approach to account for uncertainties, we integrate the SED, and calculate an apparent bolometric magnitude,  $m_{\text{bol}} = 17.71 \pm 0.03$  mag for the system.<sup>9</sup>

To determine the  $m_{\text{bol}}$  of the individual components, we can use the difference in  $BC_K$  values (Golimowski et al. 2004) of the two components and their  $K$ -band flux ratio. For SDSS J2249+0044A,  $BC_K$  varies from 3.32 to 3.34 mag for its  $L3 \pm 0.5$  spectral type. SDSS J2249+0044B ( $L5 \pm 1$ ) has possible  $BC_K$  values of 3.32–3.35 mag. Since the two components have essentially the same  $BC_K$ , the  $K$ -band flux ratio provides the bolometric flux ratio directly. We converted our measured  $K_S$ -band flux ratio ( $0.883 \pm 0.007$  mag) to a  $K$ -band flux ratio by comparing synthetic photometry (from our spatially resolved OSIRIS spectra) and derive a  $K$ -band flux ratio of  $0.893 \pm 0.007$  mag. The uncertainties for our synthetic flux ratios were small ( $< 0.2\%$ ); thus the combined uncertainty is dominated by uncertainties in our measured  $K_S$  flux ratio. From the integrated-light  $m_{\text{bol}}$  ( $17.71 \pm 0.03$  mag) and the  $K$ -band flux ratio, we calculate  $m_{\text{bol}}$ 's of  $18.11 \pm 0.03$  and  $19.00 \pm 0.03$  mag

---

<sup>9</sup> $m_{\text{bol}} = -2.5 \log f_{\text{bol}} - 18.988$  (Cushing et al. 2005) with  $f_{\text{bol}}$  expressed in units of  $W m^{-2}$

for SDSS J2249+0044A and B respectively.<sup>10</sup> Though we cannot convert  $m_{\text{bol}}$  to luminosity without a distance, the difference in  $\log(L_{\text{bol}}/L_{\odot})$ ,  $0.36 \pm 0.02$  dex, of the two components is distance independent.

### 3.4. Distance

Since SDSS J2249+0044AB shows signatures of youth, it is difficult to determine a spectroscopic distance, as absolute magnitude–SpT relations are derived only for field ( $\gtrsim 1$  Gyr old) dwarfs (e.g., Liu et al. 2006; Cruz et al. 2003). With an estimated age of  $\sim 100$  Myr, SDSS J2249+0044AB is significantly younger than the field population and may not follow the same dependence of absolute magnitude with spectral type. Nonetheless, we can use the field dwarf SpT– $BC_K$  and SpT– $M_K$  relations (Golimowski et al. 2004; Knapp et al. 2004) to compare to  $m_{\text{bol}}$ ’s of SDSS J2249+0044A and B and obtain a rough distance estimate. The expected  $M_{\text{bol}}$ ’s of L3 and L5 field dwarfs are  $14.5 \pm 0.3$  and  $15.4 \pm 0.3$  mag, corresponding to distances of  $53 \pm 7$  pc for both SDSS J2249+0044A and B.

To obtain another estimate of distance, we can compare SDSS J2249+0044AB to young objects of known distance. Jameson et al. (2008) determined the relationship between  $J - K$  color and  $M_K$  for several young associations, including the Pleiades. From their  $M_K - (J - K)$  relation for the Pleiades,<sup>11</sup> we calculate  $M_K = 11.6 \pm 0.2$  and  $11.9 \pm 0.2$  mag for SDSS J2249+0044A and B, corresponding to distances of  $44 \pm 3$  and  $58 \pm 5$  pc, respectively. We note that the reddest object used to produce the Pleiades relation of Jameson et al. (2008) has  $J - K = 1.92$ . Thus, using their relation for SDSS J2249+0044A and B ( $J - K$  of 2.01 and 2.14 mag, respectively) is an extrapolation. Jameson et al. (2008) also contain  $M_K - (J - K)$  relations for Upper Scorpius ( $\sim 5$  Myr old) and the Hyades ( $\sim 625$  Myr old), which provide us with conservative upper ( $71 \pm 7$  and  $93 \pm 11$  pc for SDSS J2249+0044A and B respectively) and lower limits ( $25 \pm 2$  and  $33 \pm 3$  pc) on the distance.

Another young object to which we can compare is G196-3B, which has a distance estimate of  $21 \pm 6$  pc based on the spectroscopic distance to G196-3A (Rebolo et al. 1998). The spectral type (L3) and near-IR colors of G196-3B ( $J - K = 2.00 \pm 0.06$  mag) are nearly iden-

---

<sup>10</sup>We also computed  $\Delta m_{\text{bol}}$  from the  $J$ -band flux ratio using an SpT– $BC_J$  relation derived from bolometric luminosities in Golimowski et al. (2004) and  $J$ -band magnitudes from Knapp et al. (2004). Unlike  $BC_K$ ,  $BC_J$  is strongly dependent on spectral type for mid-L-type dwarfs. From the range of possible spectral types for SDSS J2249+0044A and B,  $\Delta m_{\text{bol}}$  varies from 0.69 to 0.96 mag, which is consistent with the  $\Delta m_{\text{bol}}$  we determine from the  $K$ -band flux ratio.

<sup>11</sup> $M_K = 10.70 \pm 0.04 + 1.81 \pm 0.19 (J - K - 1.5)$ .

tical to those of SDSS J2249+0044A ( $L3\pm0.5$ ,  $2.01 \pm 0.08$  mag) thus we can compare their near-IR magnitudes to calculate their relative distances.<sup>12</sup> Assuming the two objects have the same age, SDSS J2249+0044A is  $2.59\pm0.05$  times more distant than G196-3B. Scaling from the distance estimate for G196-3B, we estimate that SDSS J2249+0044A has a distance of  $54\pm16$  pc. Our distance estimates from comparison to field dwarfs, Pleiades objects, and G196-3B agree to within their uncertainties. We adopt the most conservative of our distance estimates ( $54 \pm 16$  pc) as the distance to SDSS J2249+0044AB, with the caveat that this distance could be an underestimate if the system is significantly younger than the Pleiades or G196-3B. Figure 6 shows that SDSS J2249+0044A and B roughly follow the Pleiades sequence, which supports our distance determination.

At a distance of  $54\pm16$  pc, the projected physical separation of SDSS J2249+0044AB is  $17\pm5$  AU, and the luminosities ( $\log(L_{\text{bol}}/L_{\odot})$ ) of SDSS J2249+0044A and B are  $-3.9 \pm 0.3$  and  $-4.2 \pm 0.3$  dex.

### 3.5. Mass

To estimate the mass of SDSS J2249+0044A and B, we compare their luminosities and effective temperatures to predictions of evolutionary models. The SpT's of SDSS J2249+0044A and B ( $L3.0\pm0.5$  and  $L5\pm1$ ) correspond to effective temperatures ( $T_{\text{eff}}$ ) of  $1950\pm140$  and  $1700\pm160$  K using the  $SpT - T_{\text{eff}}$  relation of Golimowski et al. (2004),<sup>13</sup> with uncertainties derived from the scatter of the relation (124 K) and the uncertainty in SpTs. Figure 7 shows age versus  $T_{\text{eff}}$  and  $\log(L_{\text{bol}}/L_{\odot})$  for SDSS J2249+0044A and B with the evolutionary models of Burrows et al. (1997) overlaid. At an age of 100 Myr, the evolutionary models predict masses of  $0.029\pm0.006$  and  $0.022^{+0.006}_{-0.009} M_{\odot}$  from the luminosities of SDSS J2249+0044A and B respectively.<sup>14</sup> From the  $T_{\text{eff}}$ 's of SDSS J2249+0044A and B, the evolutionary models predict masses of  $0.030^{+0.003}_{-0.002}$  and  $0.026^{+0.002}_{-0.003} M_{\odot}$ . The masses predicted from  $T_{\text{eff}}$  and luminosity are in good agreement, which is reassuring given that the luminosities were de-

---

<sup>12</sup>To compare our (MKO) photometry of SDSS J2249+0044AB to G196-3B, we first synthesized MKO *JHK* photometry from our spectrum of G196-3B normalized to its Two Micron All Sky Survey (2MASS) *JHK* photometry. We derive MKO *JHK* magnitudes of  $14.73\pm0.05$ ,  $13.73\pm0.05$ , and  $12.73\pm0.04$  mag for G196-3B.

<sup>13</sup>Since SDSS J2249+0044A and B are young, it is possible that the field dwarf SpT- $T_{\text{eff}}$  relation will underestimate their temperatures (based on results for young objects with earlier spectral types (Luhman et al. 2003)).

<sup>14</sup>Uncertainties in the mass are determined from the uncertainties in luminosity (or  $T_{\text{eff}}$ ), and do not include age uncertainties or possible systematic errors in the evolutionary models (Dupuy et al. 2009).

terminated from the photometry of the system, whereas the  $T_{eff}$ 's are determined from the SpTs of SDSS J2249+0044A and B. Given the estimated masses of SDSS J2249+0044AB, the system will likely evolve into a late-T/Y dwarf system (Liu et al. 2010) when it reaches the typical age of the field population ( $\sim 1$  Gyr).

The uncertain age of SDSS J2249+0044AB adds additional uncertainty to the mass determinations. For an age range of 20–300 Myr, the evolutionary models predict masses ranging from 0.011 to 0.056  $M_{\odot}$  and from 0.008 to 0.050  $M_{\odot}$  for SDSS J2249+0044A and B based on their luminosities. Over the same age range, their  $T_{eff}$ 's yield possible masses of 0.013–0.050  $M_{\odot}$  and 0.012–0.045  $M_{\odot}$ . For our strict age limits (12–790 Myr), the mass of SDSS J2249+0044A could range from 0.011 to 0.070  $M_{\odot}$  and the mass of SDSS J2249+0044B could range from 0.009–0.065  $M_{\odot}$ . Thus, although their masses are very uncertain, both components are likely substellar ( $< 0.072 M_{\odot}$ ).

$\Delta \log(L_{bol}/L_{\odot})$  can be used to infer the mass ratio of a system using the analytic scaling relation from Burrows et al. (2001):  $L_{bol} \propto M^{2.64} t^{-1.3} \kappa_R^{0.35}$ . Using this relation, the well-determined  $\Delta \log(L_{bol}/L_{\odot}) = 0.36 \pm 0.02$  of SDSS J2249+0044AB corresponds to a mass ratio,  $q \equiv M_B/M_A = 0.74 \pm 0.01$ , which is lower than any known L dwarf binary.<sup>15</sup> It is important to note, however, that the Burrows et al. (2001) power-law relations are meant to describe the late-time evolution of brown dwarfs and do not fully describe younger objects. Figure 8 shows isochrones from the evolutionary models of Burrows et al. (1997). The bump in the isochrones at masses of  $\sim 0.01$ – $0.02 M_{\odot}$  is due to deuterium burning and means that  $\Delta \log(L_{bol}/L_{\odot})$  can not be used to accurately infer the mass ratio if either component is currently burning deuterium. For instance, if SDSS J2249+0044B (the less luminous component) is currently burning deuterium (age of  $\sim 140$  Myr), the mass ratio of the system could be as low as 0.4. On the other hand, if SDSS J2249+0044A (the more luminous component) is burning deuterium (age of  $\sim 75$  Myr), the mass ratio would be closer to unity, and the system could exhibit a reversal in the luminosities of the binary, with SDSS J2249+0044A being the lower mass component. The effect of deuterium burning on the evolution of brown dwarfs is discussed in detail by Saumon & Marley (2008). Unfortunately, without better constraints on the age and luminosities of SDSS J2249+0044A and B, we can not distinguish between the various mass ratio possibilities. SDSS J2249+0044AB is the first known binary system that could exhibit a flux reversal induced by deuterium burning.

---

<sup>15</sup><http://www.vlmbinaries.org>

### 3.6. Orbital Period

We have measured the projected separation of SDSS J2249+0044AB to be  $322.8 \pm 0.3$  mas, but the true semimajor axis of the binary depends on its orbital parameters. Following the method of Torres (1999), we assume random viewing angles and a uniform eccentricity distribution between  $0 < e < 1$  to derive a correction factor of  $1.10^{+0.90}_{-0.36}$  (68.3% confidence limits) to convert projected separation into a semimajor axis. At a distance of  $54 \pm 16$  pc, this results in a semimajor axis of  $19^{+17}_{-8}$  AU. For a total mass of  $0.051 M_{\odot}$  (assuming an age of  $\sim 100$  Myr old), this corresponds to an orbital period of  $400^{+600}_{-200}$  years. Unfortunately, the estimated orbital period of SDSS J2249+0044AB is too long for our two epochs of observations (Table 1) to detect any relative motion of the binary.

### 3.7. A Common Proper Motion M Dwarf

SDSS J2249+0044AB lies within the SDSS region known as Stripe 82, which is a  $2^{\circ}5$  wide strip spanning  $99^{\circ}$  of the celestial equator. Bramich et al. (2008) analyzed all available observations of this region spanning the seven years of survey operations from 1998 to 2005, computing light curves and proper motions on an extragalactic reference frame from catalog data. They computed a proper motion of  $\mu = 82.8 \pm 3.7$  mas yr $^{-1}$  at a P.A. of  $85^{\circ}4 \pm 2^{\circ}5$  for SDSS J2249+0044AB.<sup>16</sup> We searched the light-motion catalog for any other objects with a well-detected proper motion ( $\sigma_{\mu}/\mu > 10$  and  $\sigma_{\text{PA}} < 10$  deg) that share similar motion (both  $\mu$  and PA within  $3\sigma$ ) with SDSS J2249+0044AB. We found one such object within a limit of  $700''$  of SDSS J2249+0044AB ( $3.8 \times 10^4$  AU at 54 pc, i.e., well beyond the wide binary cutoff of  $10^4$  AU found in simulations by Weinberg et al. (1987)). This common proper motion companion is GSC 00568-01752, which lies  $48^{\circ}937 \pm 0^{\circ}009$  at a PA of  $257^{\circ}04 \pm 0^{\circ}01$  away from SDSS J2249+0044AB (a projected separation of  $2600 \pm 800$  AU for  $d=54 \pm 16$  pc) and has a proper motion of  $\mu = 90.7 \pm 3.3$  mas yr $^{-1}$  and PA= $87^{\circ}0 \pm 2^{\circ}1$ , in agreement with the proper motion of SDSS J2249+0044AB at  $1.6\sigma$  and  $0.5\sigma$ , respectively.

By comparing the SDSS and 2MASS photometry of GSC 00568-01752<sup>17</sup> with colors for field M dwarfs (West et al. 2008), we determine a spectral type of  $M2 \pm 2$  via  $\chi^2$  minimization. From the  $i - z$  photometric parallax relation of West et al. (2005), we calculate a distance of  $53 \pm 15$  pc for GSC 00568-01752, in excellent agreement with our distance estimate for

---

<sup>16</sup>We note that the proper motion calculated by Bramich et al. (2008) agrees to within the uncertainties with other recent measurements (Scholz et al. 2009; Faherty et al. 2008).

<sup>17</sup> $r=13.63 \pm 0.01$ ,  $i=12.45 \pm 0.01$ ,  $z=11.93 \pm 0.01$ ,  $J=10.35 \pm 0.03$ ,  $H=8.74 \pm 0.03$ , and  $K=9.51 \pm 0.023$  mag.

SDSS J2249+0044AB. GSC 00568-01752 has a low S/N X-ray detection in the *ROSAT* All-Sky Survey (1RXS J224957.2+004402; Micaelian et al. 2006) from which we calculate  $F_X$  using the count rate to flux conversion of Schmitt et al. (1995). We determine  $\log(F_X/F_J) = -2.3 \pm 0.3^{18}$  for GSC 00568-01752 which is consistent with values for young ( $\lesssim 650$  Myr old) nearby M dwarfs (Shkolnik et al. 2009) and provides additional evidence that GSC 00568-01752 and SDSS J2249+0044AB are associated. Further study of GSC 00568-01752 could help to constrain the age and distance of SDSS J2249+0044AB.

### 3.8. Moving Group Membership

Young moving groups and associations are loose groups of stars sharing common ages, compositions, and kinematics. Thus, membership of SDSS J2249+0044AB in a young moving group would provide an independent estimate of age and metallicity. Membership in a young moving group is typically confirmed via common space motion ( $UVW$ ), which requires knowledge of the object’s distance, proper motion, and radial velocity. Using the photometric distance estimate of SDSS J2249+0044AB ( $54 \pm 16$  pc) and its proper motion ( $\mu = 82.8 \pm 3.7$  mas yr $^{-1}$  and PA= $85^\circ.4 \pm 2^\circ.5$ ; Bramich et al. 2008), we calculated its range of possible  $UVW$  for radial velocities from  $-50$  to  $50$  km s $^{-1}$ . Figure 9 shows the possible space motion of SDSS J2249+0044AB compared to known moving groups (Torres et al. 2008; Zuckerman & Song 2004). Only two groups, the Octans ( $\sim 20$  Myr old) and Argus ( $\sim 40$  Myr old) associations, have  $UVW$  that overlap the  $1\sigma$  range of SDSS J2249+0044AB. Both of these young groups, however, are concentrated far in the southern hemisphere (Figure 10), making membership with SDSS J2249+0044AB unlikely. SDSS J2249+0044AB could be an isolated young field object. Radial velocity and parallax measurements for SDSS J2249+0044AB are necessary to further assess possible membership with young moving groups.

## 4. Conclusions

As a part of our Keck LGS AO survey of young field brown dwarfs, we have discovered the young L dwarf, SDSS J2249+0044AB to be a  $0''.32$  binary. Over our two epochs of imaging spanning nearly two years, the separation and P.A. of the system do not change significantly, indicating that SDSS J2249+0044A and B are comoving and thus physically

---

<sup>18</sup>Our calculation of  $F_J$  uses a  $J$ -band flux density for Vega of  $3.129 \pm 0.055 \times 10^{-13}$  W cm $^{-2}$   $\mu\text{m}^{-1}$  (Cohen et al. 2003) and a bandwidth of  $0.29 \mu\text{m}$

associated. Using spatially resolved  $K$ -band spectroscopy, we determine spectral types of  $L3\pm0.5$  and  $L5\pm1$  for SDSS J2249+0044A and B, respectively. SDSS J2249+0044A and B have unusually red near-IR colors relative to field dwarfs, which can indicate either a young age or a dusty photosphere. The FeH, K I, and Na I absorption features in the near-IR spectrum of SDSS J2249+0044AB are weaker and the VO absorption is stronger than seen in normal and dusty photosphere L dwarf spectra, indicating a young age for SDSS J2249+0044AB. The  $K-L'$  colors of SDSS J2249+0044A and B are significantly redder than 2MASS 2224-0158, a dusty L4.5 dwarf, hinting that  $K-L'$  color can be used to distinguish between young and dusty objects. The near-IR spectra of SDSS J2249+0044AB and G196-3B (a young L3 dwarf) are remarkably similar, thus we adopt an age of 100 Myr for SDSS J2249+0044AB, but note that ages of 12-790 Myr are possible. By comparing the  $K$ -band magnitude of SDSS J2249+0044A to that of G196-3B (which has a distance estimate from the spectroscopic distance of G196-3A), we estimate a distance of  $54\pm16$  pc for the system.

Comparison of the luminosities of SDSS J2249+0044A and B to evolutionary models for an age of 100 Myr yields masses of  $0.029\pm0.006$  and  $0.021_{-0.009}^{+0.006} M_{\odot}$  respectively. For ages of 12–790 Myr, the masses could range from 0.011 to  $0.070 M_{\odot}$  for SDSS J2249+0044A and from 0.009 to  $0.065 M_{\odot}$  for SDSS J2249+0044B. Thus, SDSS J2249+0044A and B are clearly substellar. Evolutionary models predict that for the range of possible ages and luminosities either component could be burning deuterium. The mass ratios of the binary could range from 0.4 to near unity depending on which component is burning deuterium. The system is the first known binary which could exhibit a flux reversal due to deuterium burning. For a range of plausible radial velocities, we show that the position, proper motion, and distance to the system are inconsistent with membership in known young moving groups. A common proper motion search of SDSS stripe 82 shows that GSC 00568-01752 (which has colors consistent with an early M dwarf) is likely associated with SDSS J2249+0044AB, and further study of this M dwarf could help to better constrain the age, distance and kinematics of SDSS J2249+0044AB. As a young, low-mass system having very red near-IR colors, SDSS J2249+0044AB is a valuable template for future studies of planetary-mass objects. Better constraints on the age, luminosities, and effective temperatures of SDSS J2249+0044A and B could provide critical tests to evolutionary models for young L dwarfs.

We gratefully acknowledge the Keck LGS AO team for their exceptional efforts in bringing the LGS AO system to fruition. It is a pleasure to thank Randy Campbell, Jim Lyke, Al Conrad, Hien Tran, Christine Melcher, Cindy Wilburn, Joel Aycock, Jason McElroy, and the Keck Observatory staff for assistance with the observations. This publication benefited from helpful discussions with Kevin Marshall and Evgenya Shkolnik regarding *ROSAT*

data. We sincerely thank Eric Mamajek for informing us about GSC 00568-01752, the possible M dwarf companion to SDSS J2249+0044AB. We also thank John Rayner and the IRTF Observatory staff for assistance with our SpeX observations and data reduction. This publication has made use of the VLM Binaries Archive maintained by Nick Siegler at <http://www.vlmbinaries.org>. This research has benefitted from the M, L, and T dwarf compendium housed at DwarfArchives.org and maintained by Chris Gelino, Davy Kirkpatrick, and Adam Burgasser as well as from the SpeX Prism Spectral Libraries, maintained by Adam Burgasser at <http://www.browndwarfs.org/spexprism>. M.C.L., K.N.A. and T.J.D. acknowledge support for this work from NSF grant AST-0507833 and AST-0407441. M.C.L. also acknowledges support from an Alfred P. Sloan Research Fellowship. K.N.A. was partially supported by NASA Origins of Solar Systems grant NNX07AI83G.

## REFERENCES

- Allers, K. N., Kessler-Silacci, J. E., Cieza, L. A., & Jaffe, D. T. 2006, *ApJ*, 644, 364
- Allers, K. N., et al. 2007, *ApJ*, 657, 511
- Allers, K. N., et al. 2009, *ApJ*, 697, 824
- Baraffe, I., Chabrier, G., Barman, T. S., Allard, F., & Hauschildt, P. H. 2003, *A&A*, 402, 701
- Barnes, S. A. 2007, *ApJ*, 669, 1167
- Biller, B. A., & Close, L. M. 2007, *ApJ*, 669, L41
- Bramich, D. M., et al. 2008, *MNRAS*, 386, 887
- Burgasser, A. J. 2007, *ApJ*, 659, 655
- Burgasser, A. J., Reid, I. N., Siegler, N., Close, L., Allen, P., Lowrance, P., & Gizis, J. 2007, *Protostars and Planets V*, 427
- Burrows, A., Hubbard, W. B., Lunine, J. I., & Liebert, J. 2001, *Reviews of Modern Physics*, 73, 719
- Burrows, A., et al. 1997, *ApJ*, 491, 856
- Casewell, S. L., Dobbie, P. D., Hodgkin, S. T., Moraux, E., Jameson, R. F., Hambly, N. C., Irwin, J., & Lodieu, N. 2007, *MNRAS*, 378, 1131

- Chauvin, G., Lagrange, A.-M., Dumas, C., Zuckerman, B., Mouillet, D., Song, I., Beuzit, J.-L., & Lowrance, P. 2004, *A&A*, 425, L29
- Chauvin, G., Lagrange, A.-M., Dumas, C., Zuckerman, B., Mouillet, D., Song, I., Beuzit, J.-L., & Lowrance, P. 2005, *A&A*, 438, L25
- Cohen, M., Wheaton, W. A., & Megeath, S. T. 2003, *AJ*, 126, 1090
- Cruz, K. L., Kirkpatrick, J. D., & Burgasser, A. J. 2009, *AJ*, 137, 3345
- Cruz, K. L., Reid, I. N., Liebert, J., Kirkpatrick, J. D., & Lowrance, P. J. 2003, *AJ*, 126, 2421
- Cushing, M. C., Rayner, J. T., & Vacca, W. D. 2005, *ApJ*, 623, 1115
- Cushing, M. C., Vacca, W. D., & Rayner, J. T. 2004, *PASP*, 116, 362
- Dupuy, T. J., Liu, M. C., & Ireland, M. J. 2009, *ApJ*, 692, 729
- Faherty, J. K., Burgasser, A. J., Cruz, K. L., Shara, M. M., Walter, F. M., & Gelino, C. R. 2008, arXiv:0809.3008
- Fortney, J. J., Marley, M. S., Saumon, D., & Lodders, K. 2008, *ApJ*, 683, 1104
- Geballe, T. R., et al. 2002, *ApJ*, 564, 466
- Ghez, A. M., et al. 2008, *ApJ*, 689, 1044
- Golimowski, D. A., et al. 2004, *AJ*, 127, 3516
- Gorlova, N. I., Meyer, M. R., Rieke, G. H., & Liebert, J. 2003, *ApJ*, 593, 1074
- Goto, M., et al. 2002, *ApJ*, 567, L59
- Hawley, S. L., et al. 2002, *AJ*, 123, 3409
- Jameson, R. F., Lodiou, N., Casewell, S. L., Bannister, N. P., & Dobbie, P. D. 2008, *MNRAS*, 385, 1771
- Kalas, P., et al. 2008, *Science*, 322, 1345
- Kirkpatrick, J. D., Barman, T. S., Burgasser, A. J., McGovern, M. R., McLean, I. S., Tinney, C. G., & Lowrance, P. J. 2006, *ApJ*, 639, 1120
- Kirkpatrick, J. D., Dahn, C. C., Monet, D. G., Reid, I. N., Gizis, J. E., Liebert, J., & Burgasser, A. J. 2001, *AJ*, 121, 3235

- Kirkpatrick, J. D., et al. 2000, *AJ*, 120, 447
- Kirkpatrick, J. D., et al. 2008, *ApJ*, 689, 1295
- Knapp, G. R., et al. 2004, *AJ*, 127, 3553
- Krabbe, A., Gasaway, T., Song, I., Iserlohe, C., Weiss, J., Larkin, J. E., Barczys, M., & Lafreniere, D. 2004, *Proc. SPIE*, 5492, 1403
- Larkin, J. E., et al. 2003, *Proc. SPIE*, 4841, 1600
- Leggett, S. K., et al. 2002, *ApJ*, 564, 452
- Liu, M. C., & Leggett, S. K. 2005, *ApJ*, 634, 616
- Liu, M. C., Leggett, S. K., Golimowski, D. A., Chiu, K., Fan, X., Geballe, T. R., Schneider, D. P., & Brinkmann, J. 2006, *ApJ*, 647, 1393
- Liu, M. C., Leggett, S. K., & Dupuy, T. J., 2010, *ApJ*, *submitted*
- Looper, D. L., et al. 2008, *ApJ*, 686, 528
- Lucas, P. W., Roche, P. F., Allard, F., & Hauschildt, P. H. 2001, *MNRAS*, 326, 695
- Lucas, P. W., Weights, D. J., Roche, P. F., & Riddick, F. C. 2006, *MNRAS*, 373, L60
- Luhman, K. L., Mamajek, E. E., Allen, P. R., & Cruz, K. L. 2009, *ApJ*, 703, 399
- Luhman, K. L., Stauffer, J. R., Muench, A. A., Rieke, G. H., Lada, E. A., Bouvier, J., & Lada, C. J. 2003, *ApJ*, 593, 1093
- Mamajek, E. E., & Hillenbrand, L. A. 2008, *ApJ*, 687, 1264
- Mamajek, E. E., & Meyer, M. R. 2007, *ApJ*, 668, L175
- Marois, C., Macintosh, B., Barman, T., Zuckerman, B., Song, I., Patience, J., Lafrenière, D., & Doyon, R. 2008, *Science*, 322, 1348
- McLean, I. S., McGovern, M. R., Burgasser, A. J., Kirkpatrick, J. D., Prato, L., & Kim, S. S. 2003, *ApJ*, 596, 561
- Mentuch, E., Brandeker, A., van Kerkwijk, M. H., Jayawardhana, R., & Hauschildt, P. H. 2008, *ApJ*, 689, 1127
- Mickaelian, A. M., Hovhannisyanyan, L. R., Engels, D., Hagen, H.-J., & Voges, W. 2006, *A&A*, 449, 425

- Mohanty, S., Jayawardhana, R., Huélamo, N., & Mamajek, E. 2007, *ApJ*, 657, 1064
- Montes, D., López-Santiago, J., Gálvez, M. C., Fernández-Figueroa, M. J., De Castro, E., & Cornide, M. 2001, *MNRAS*, 328, 45
- Muench, A. A., Lada, C. J., Luhman, K. L., Muzerolle, J., & Young, E. 2007, *AJ*, 134, 411
- Nakajima, T., Tsuji, T., & Yanagisawa, K. 2004, *ApJ*, 607, 499
- Patten, B. M., et al. 2006, *ApJ*, 651, 502
- Potter, D., Martín, E. L., Cushing, M. C., Baudoz, P., Brandner, W., Guyon, O., & Neuhauser, R. 2002, *ApJ*, 567, L133
- Rayner, J. T., Toomey, D. W., Onaka, P. M., Denault, A. J., Stahlberger, W. E., Vacca, W. D., Cushing, M. C., & Wang, S. 2003, *PASP*, 115, 362
- Rebolo, R., Zapatero Osorio, M. R., Madrugá, S., Bejar, V. J. S., Arribas, S., & Licandro, J. 1998, *Science*, 282, 1309
- Reid, I. N., Burgasser, A. J., Cruz, K. L., Kirkpatrick, J. D., & Gizis, J. E. 2001a, *AJ*, 121, 1710
- Reid, I. N., Cruz, K. L., Kirkpatrick, J. D., Allen, P. R., Mungall, F., Liebert, J., Lowrance, P., & Sweet, A. 2008, *AJ*, 136, 1290
- Reid, I. N., Gizis, J. E., Kirkpatrick, J. D., & Koerner, D. W. 2001b, *AJ*, 121, 489
- Saumon, D., & Marley, M. S. 2008, *ApJ*, 689, 1327
- Schmitt, J. H. M. M., Fleming, T. A., & Giampapa, M. S. 1995, *ApJ*, 450, 392
- Scholz, R.-D., Storm, J., Knapp, G. R., & Zinnecker, H. 2009, *A&A*, 494, 949
- Shkolnik, E., Liu, M. C., & Reid, I. N. 2009, *ApJ*, 699, 649
- Simons, D. A., & Tokunaga, A. 2002, *PASP*, 114, 169
- Slesnick, C. L., Hillenbrand, L. A., & Carpenter, J. M. 2004, *ApJ*, 610, 1045
- Song, I., Schneider, G., Zuckerman, B., Farihi, J., Becklin, E. E., Bessell, M. S., Lowrance, P., & Macintosh, B. A. 2006, *ApJ*, 652, 724
- Testi, L., et al. 2001, *ApJ*, 552, L147

- Tokunaga, A. T., & Kobayashi, N. 1999, *AJ*, 117, 1010
- Tokunaga, A. T., Simons, D. A., & Vacca, W. D. 2002, *PASP*, 114, 180
- Tokunaga, A. T., & Vacca, W. D. 2005, *PASP*, 117, 1459
- Torres, C. A. O., Quast, G. R., Melo, C. H. F., & Sterzik, M. F. 2008, *Handbook of Star Forming Regions, Volume II: The Southern Sky ASP Monograph Publications, Vol. 5. Edited by Bo Reipurth, p.757*
- Torres, G. 1999, *PASP*, 111, 169
- Vacca, W. D., Cushing, M. C., & Rayner, J. T. 2003, *PASP*, 115, 389
- van Dam, M. A., et al. 2006, *PASP*, 118, 310
- Weinberg, M. D., Shapiro, S. L., & Wasserman, I. 1987, *ApJ*, 312, 367
- West, A. A., Hawley, S. L., Bochanski, J. J., Covey, K. R., Reid, I. N., Dhital, S., Hilton, E. J., & Masuda, M. 2008, *AJ*, 135, 785
- West, A. A., Walkowicz, L. M., & Hawley, S. L. 2005, *PASP*, 117, 706
- Wizinowich, P. L., et al. 2006, *PASP*, 118, 297
- Zuckerman, B., & Song, I. 2004, *ARA&A*, 42, 685
- Zuckerman, B., Song, I., Bessell, M. S., & Webb, R. A. 2001, *ApJ*, 562, L87

Table 1. Keck LGS AO Observations

| Date<br>(UT) | Instrument | Airmass | Filter               | FWHM<br>(mas)   | Strehl Ratio <sup>a</sup> | $\rho$<br>(mas) | P.A.<br>(deg) | Flux Ratio<br>(mag) |
|--------------|------------|---------|----------------------|-----------------|---------------------------|-----------------|---------------|---------------------|
| 2006 Oct 14  | NIRC2      | 1.07    | <i>J</i>             | 61±7            | 0.048±0.009               | 322.0±1.0       | 279.53±0.08   | 1.024±0.016         |
|              | NIRC2      | 1.07    | <i>H</i>             | 56±6            | 0.13±0.03                 | 322.8±0.3       | 279.49±0.03   | 0.953±0.009         |
|              | NIRC2      | 1.06    | <i>K<sub>S</sub></i> | 57±3            | 0.31±0.06                 | 322.8±0.3       | 279.50±0.04   | 0.883±0.007         |
| 2008 Sep 8   | NIRC2      | 1.06    | <i>L'</i>            | 93 <sup>b</sup> | 0.22 <sup>b</sup>         | 320.8±0.8       | 280.9±0.3     | 0.60±0.05           |
| 2008 Sep 9   | OSIRIS     | 1.35    | <i>Zbb</i>           | 130±20          | 0.015 <sup>b</sup>        | 309±7           | 281.5±0.8     | 1.12±0.04           |
|              | OSIRIS     | 1.43    | <i>Hn1</i>           | 95±12           | 0.047 <sup>b</sup>        | 307±6           | 281.0±0.5     | 1.02±0.04           |

<sup>a</sup>For NIRC2 images, Strehl ratios were computed using the publicly available routine NIRC2STREHL.

<sup>b</sup>These values are measured from the stacked mosaic of individual dithers and thus do not have rms errors.

Table 2. Photometry of SDSS J2249+0044AB

| Band  | $A + B$<br>(mag)   | $A$<br>(mag)       | $B$<br>(mag)       |
|-------|--------------------|--------------------|--------------------|
| $i$   | $21.64 \pm 0.05^a$ | ...                | ...                |
| $z$   | $19.48 \pm 0.02^a$ | ...                | ...                |
| $Z$   | $18.24 \pm 0.05^b$ | ...                | ...                |
| $Zbb$ | $17.33 \pm 0.05^c$ | $17.66 \pm 0.05$   | $18.78 \pm 0.06$   |
| $J$   | $16.47 \pm 0.07^d$ | $16.83 \pm 0.07$   | $17.85 \pm 0.07$   |
| $Hn1$ | $15.98 \pm 0.05^c$ | $16.34 \pm 0.05$   | $17.36 \pm 0.06$   |
| $H$   | $15.36 \pm 0.03^d$ | $15.74 \pm 0.04$   | $16.69 \pm 0.04$   |
| $K$   | $14.42 \pm 0.03^d$ | $14.82 \pm 0.03^e$ | $15.71 \pm 0.03^e$ |
| $L'$  | $12.71 \pm 0.07^f$ | $13.20 \pm 0.07$   | $13.80 \pm 0.07$   |
| [3.6] | $13.24 \pm 0.05$   | ...                | ...                |
| [4.5] | $13.07 \pm 0.05$   | ...                | ...                |
| [5.8] | $12.73 \pm 0.05$   | ...                | ...                |
| [8.0] | $12.55 \pm 0.05$   | ...                | ...                |

<sup>a</sup>from Scholz et al. (2009) in SDSS magnitude and filter systems

<sup>b</sup>from Leggett et al. (2002)

<sup>c</sup>synthesized from our SpeX spectrum

<sup>d</sup>weighted mean of values reported in Table 9 of Knapp et al. (2004)

<sup>e</sup> $K_S$ -band flux ratio ( $0.883 \pm 0.007$  mag) converted to  $K$ -band flux ratio ( $0.893 \pm 0.007$  mag) by synthesizing  $K$ -band photometry from our OSIRIS spectra

<sup>f</sup>from Golimowski et al. (2004)

Table 3. *K*-band Spectral Indices

| Index                          | Reference                                | SDSS J2249+0044A   |                  | SDSS J2249+0044B   |                  |
|--------------------------------|--|--------------------|------------------|--------------------|------------------|
|                                |  | Value <sup>a</sup> | SpT <sup>b</sup> | Value <sup>a</sup> | SpT <sup>b</sup> |
| CH <sub>4</sub> 2.2 $\mu$ m    | Geballe et al. (2002)                    | 0.941 $\pm$ 0.003  | L3.5 $\pm$ 0.5   | 1.047 $\pm$ 0.006  | L6.0 $\pm$ 0.5   |
| H <sub>2</sub> O–2             | Slesnick et al. (2004) <sup>c</sup>      | 0.799 $\pm$ 0.006  | L2.5 $\pm$ 1.5   | ...                | ...              |
| K1                             | Tokunaga & Kobayashi (1999) <sup>d</sup> | 0.238 $\pm$ 0.006  | L2.4 $\pm$ 0.9   | 0.21 $\pm$ 0.01    | L1.8 $\pm$ 1.0   |
| H <sub>2</sub> OD              | McLean et al. (2003)                     | 0.85 $\pm$ 0.07    | L3.3 $\pm$ 1.8   | 0.85 $\pm$ 0.11    | L3.2 $\pm$ 2.9   |
| sH <sub>2</sub> O <sup>K</sup> | Testi et al. (2001)                      | 0.27 $\pm$ 0.01    | L2.3 $\pm$ 1.0   | 0.30 $\pm$ 0.05    | L2.9 $\pm$ 1.0   |

<sup>a</sup>Using a Monte Carlo approach to account for uncertainties in the spectra

<sup>b</sup>Using a Monte Carlo approach to account for uncertainties in spectra and the index-SpT relation

<sup>c</sup>valid for spectral types of M2–L3, thus the measurement for SDSS J2249+0044B is omitted.

<sup>d</sup>Index–SpT relation from Reid et al. (2001b)

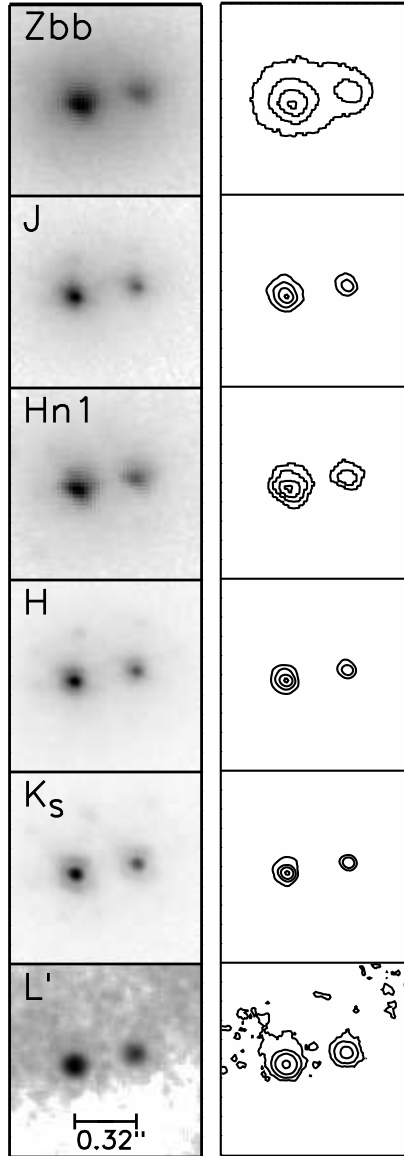


Fig. 1.— Imaging of SDSS J2249+0044AB from Keck LGS AO. North is up and east is left. Each image is  $0''.75$  on a side. The grayscale image uses a square-root intensity stretch. Contours are drawn from 90%, 45%, 22.5%, and 11.2% of the peak value in each bandpass.

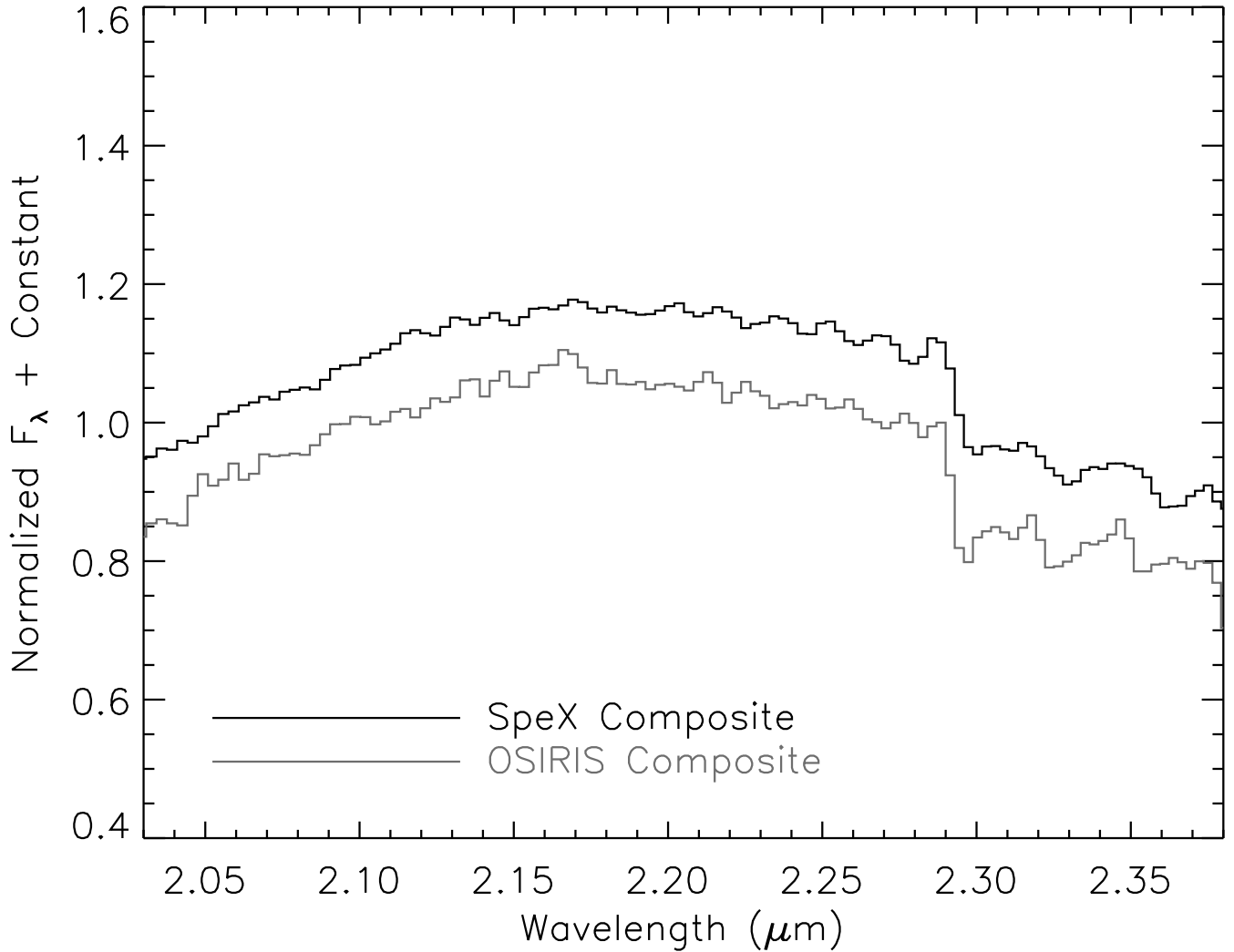


Fig. 2.— Composite K-band spectra of SDSS J2249+0044AB. Both spectra have been normalized by their medians, and the SpeX integrated-light spectrum (black) has been offset by 0.1. The Keck II/OSIRIS composite spectrum (gray) was created by flux calibrating the individual spectra of SDSS J2249+0044A and B using the magnitudes in Table 2, adding the spectra together and smoothing to the SpeX prism resolution ( $R \sim 150$ ). There is good agreement between the two spectra, indicating that our spectral extraction and telluric correction yield consistent results.

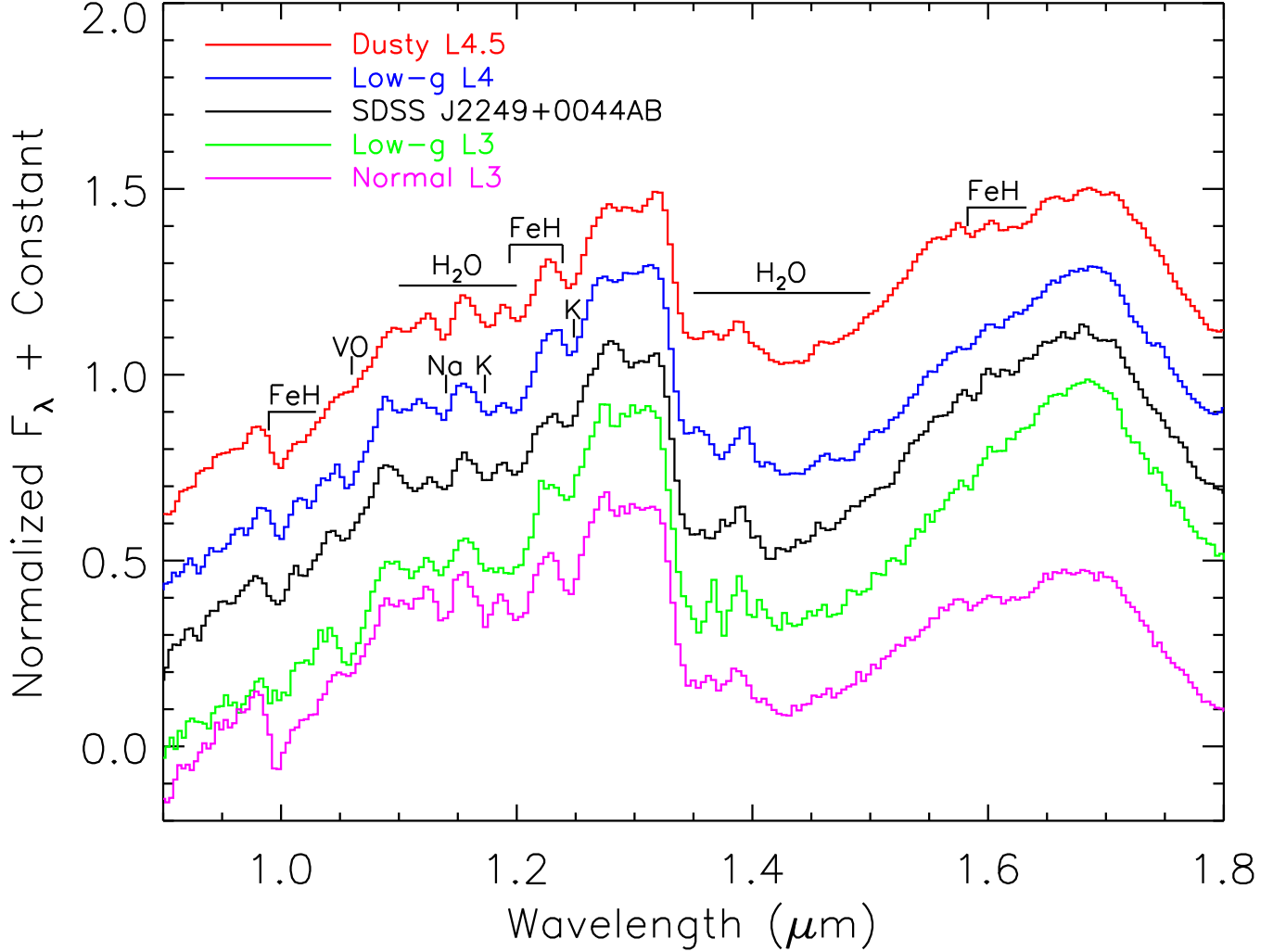


Fig. 3.— Composite near-IR spectrum of SDSS J2249+0044AB (black), compared to an L4.5 dwarf with a dusty photosphere (2MASS 2224-0158, red), a low-gravity L4 dwarf (2MASS 0501-0010, blue), a low-gravity L3 dwarf (G196-3B, green), and a normal field L3 dwarf (2MASS 1506+1321; Burgasser et al. 2007, magenta). The spectra are median-normalized and offset by constants (in intervals of 0.2). The FeH, K I, and Na I absorption features in the spectrum of SDSS J2249+0044AB are weaker and the VO absorption is stronger than seen in the normal and dusty L dwarf spectra, indicating a low-gravity (and hence young age) for SDSS J2249+0044AB.

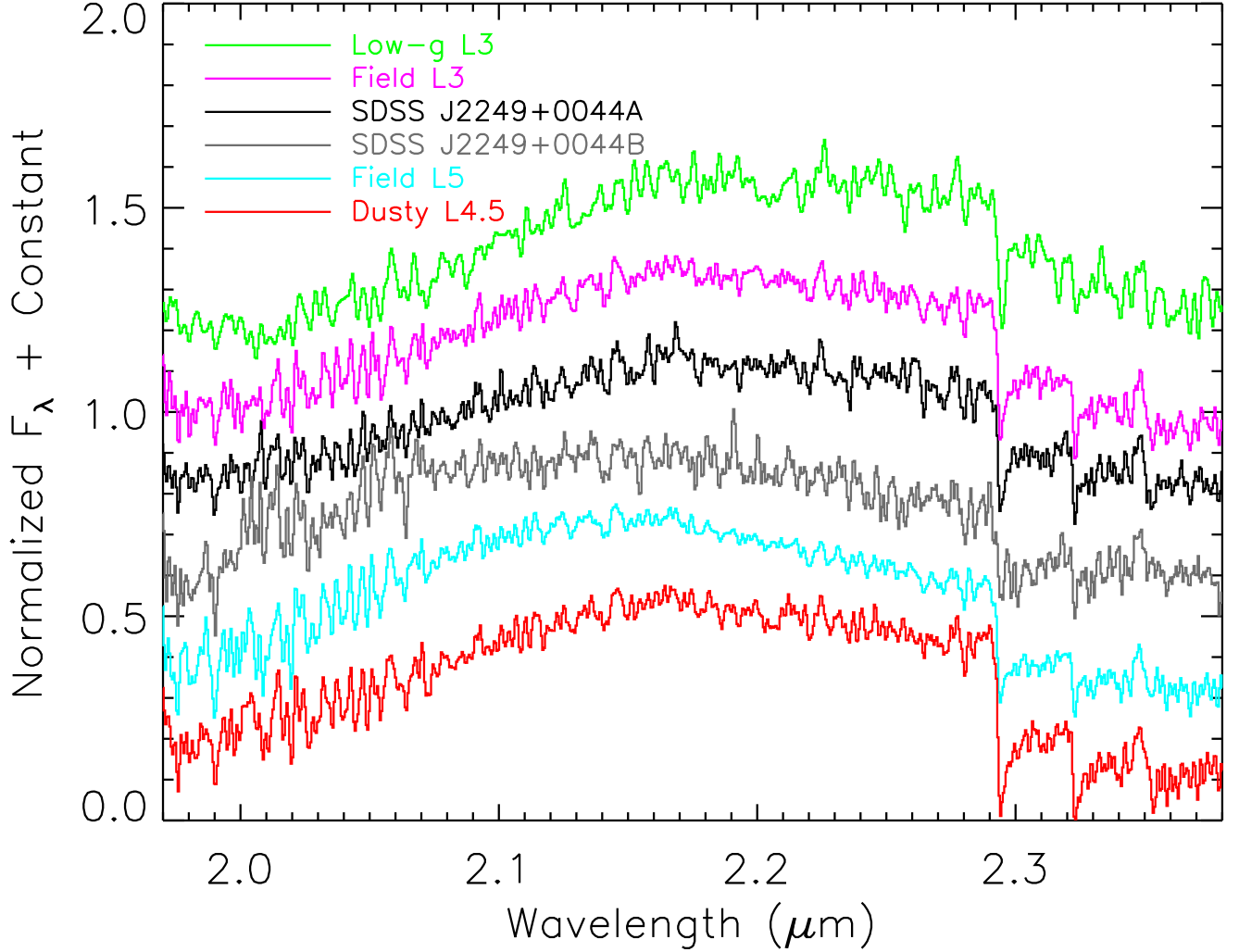


Fig. 4.— Keck II/OSIRIS  $K$ -band spectra of SDSS J2249+0044A and B, compared to IRTF/SpeX spectra of a low-gravity L3 dwarf (G196-3B, green), a field L3 dwarf (2MASS 1506+1321, magenta), a field L5 dwarf (2MASS 1507-1627, cyan) and an L4.5 dwarf with a dusty photosphere (2MASS 2224-0158, red). The spectra of SDSS J2249+0044A and B have been smoothed to the SpeX spectral resolution ( $R \sim 2000$ ). The spectra of field and dusty dwarfs are from Cushing et al. (2005), and the G196-3B spectrum is from Allers et al. (2007).

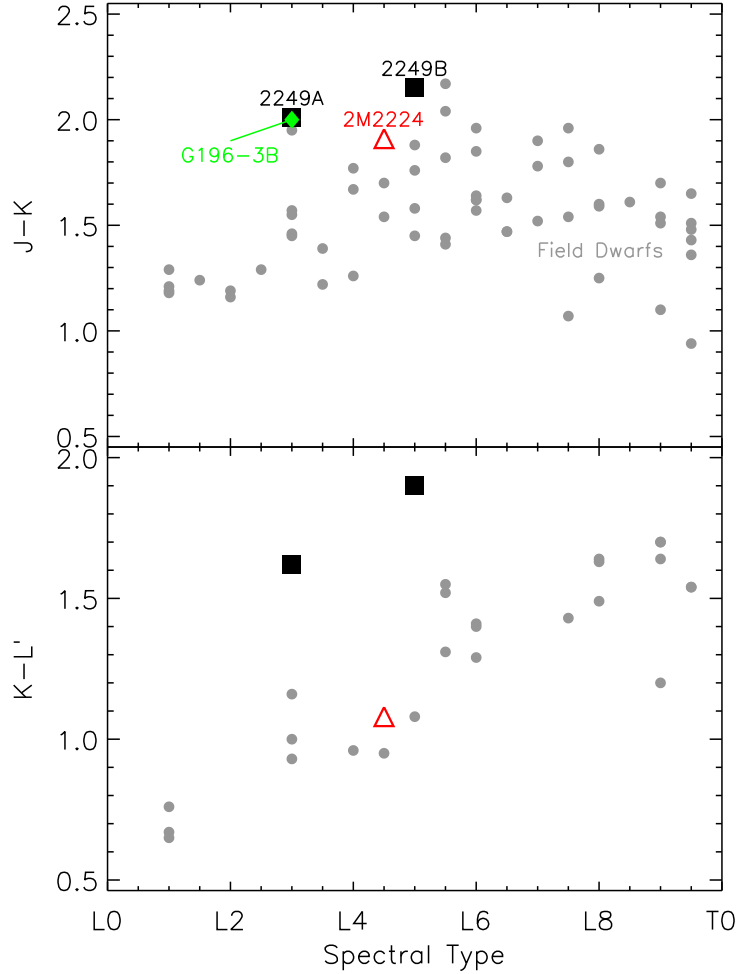


Fig. 5.— MKO  $J-K$  (top) and  $K-L'$  (bottom) colors as a function of spectral type for L dwarfs. Field dwarf  $J-K$  colors (Knapp et al. 2004) and  $K-L'$  colors (Golimowski et al. 2004) are shown as gray circles. The black squares show the colors of SDSS J2249+0044A and B (Table 2). The green diamond shows the color of G196-3B, a  $\sim 100$  Myr L3 dwarf (Cruz et al. 2009), synthesized from its near-IR spectrum. The open red triangles show the colors of 2MASS 2224-0158 (Knapp et al. 2004; Golimowski et al. 2004), an L4.5 field dwarf with a dusty photosphere (Kirkpatrick et al. 2000; Cushing et al. 2005). SDSS J2249+0044A and B have red colors compared to normal field dwarfs of the same spectral type, which could be due to a low surface gravity (youth) or a dusty photosphere.

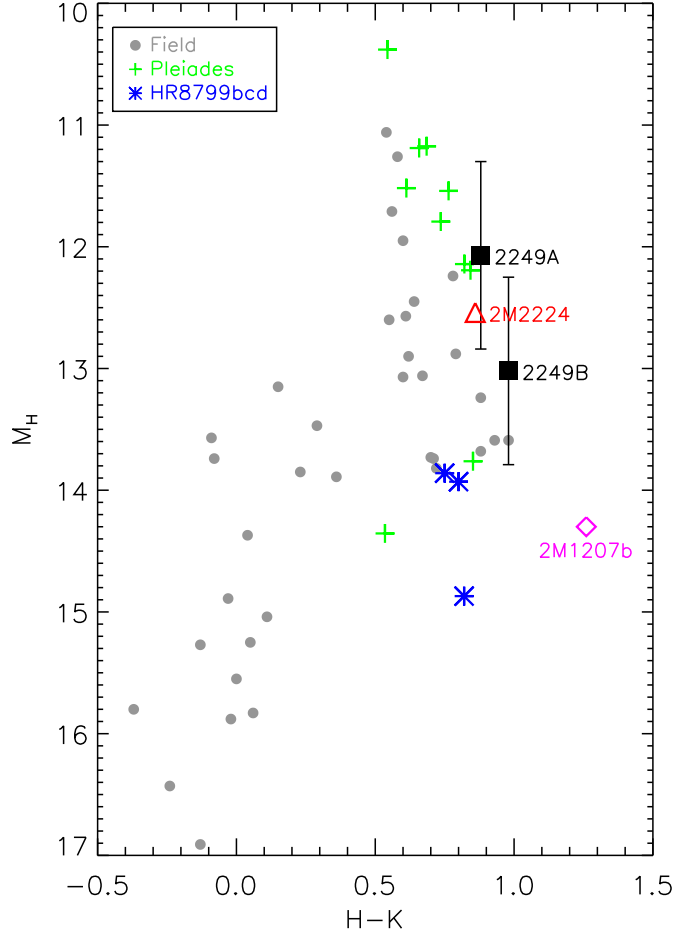


Fig. 6.— MKO  $H - K$  color versus  $H$ -band absolute magnitude for L and T dwarfs. The black squares show photometry of SDSS J2249+0044A and B based on our photometric distance estimate of  $54 \pm 16$  pc. Field objects (Knapp et al. 2004) are displayed as gray circles and Pleiades candidates from Casewell et al. (2007) are displayed as green crosses. For reference, we also plot photometry of the HR 8799 planets (blue asterisks; Marois et al. 2008), the young planetary-mass object 2MASS 1207b (magenta diamond; Chauvin et al. 2004; Mohanty et al. 2007; Biller & Close 2007), and the dusty field L dwarf 2MASS 2224–0158 (red triangle; Knapp et al. 2004). SDSS J2249+0044AB appears to follow the Pleiades sequence, which supports our age and distance determination. Note that the young planetary-mass objects are somewhat underluminous compared to the field sequence, though not as dramatically as indicated by a similar version of this plot in Marois et al. (2008) (the difference in the two plots arises from a plotting error in the field object absolute magnitudes in the Marois et al. plot (T. S. Barman, private communication)).

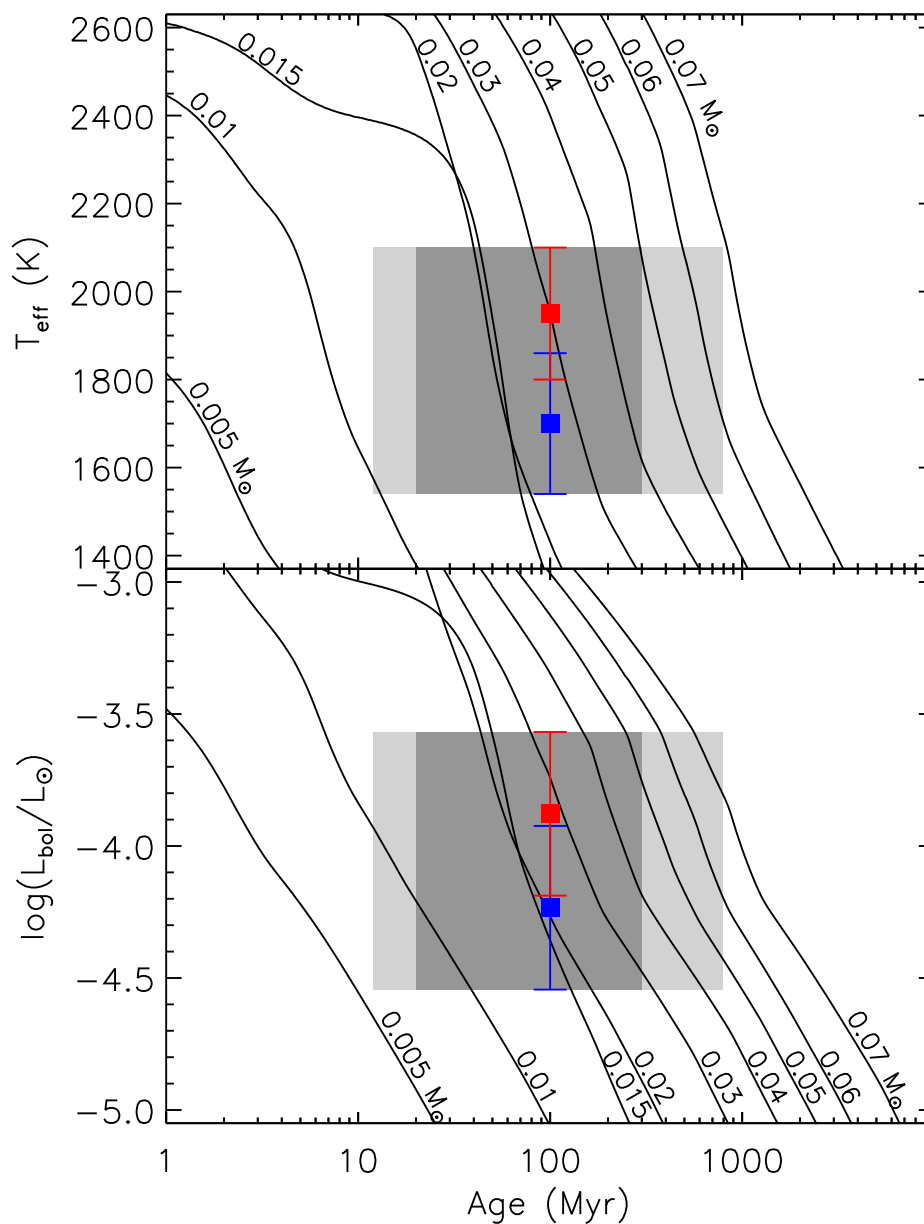


Fig. 7.— Plot of age vs. effective temperature (top) and  $\log(L_{\text{bol}}/L_{\odot})$  (bottom) for SDSS J2249+0044A and B with model iso-mass contours from Burrows et al. (1997) overlaid. The shaded regions show the range of possible ages for SDSS J2249+0044AB from our strict age limits (12-790 Myr; light gray shading) and the age of G196-3B (20-300 Myr; gray shading).

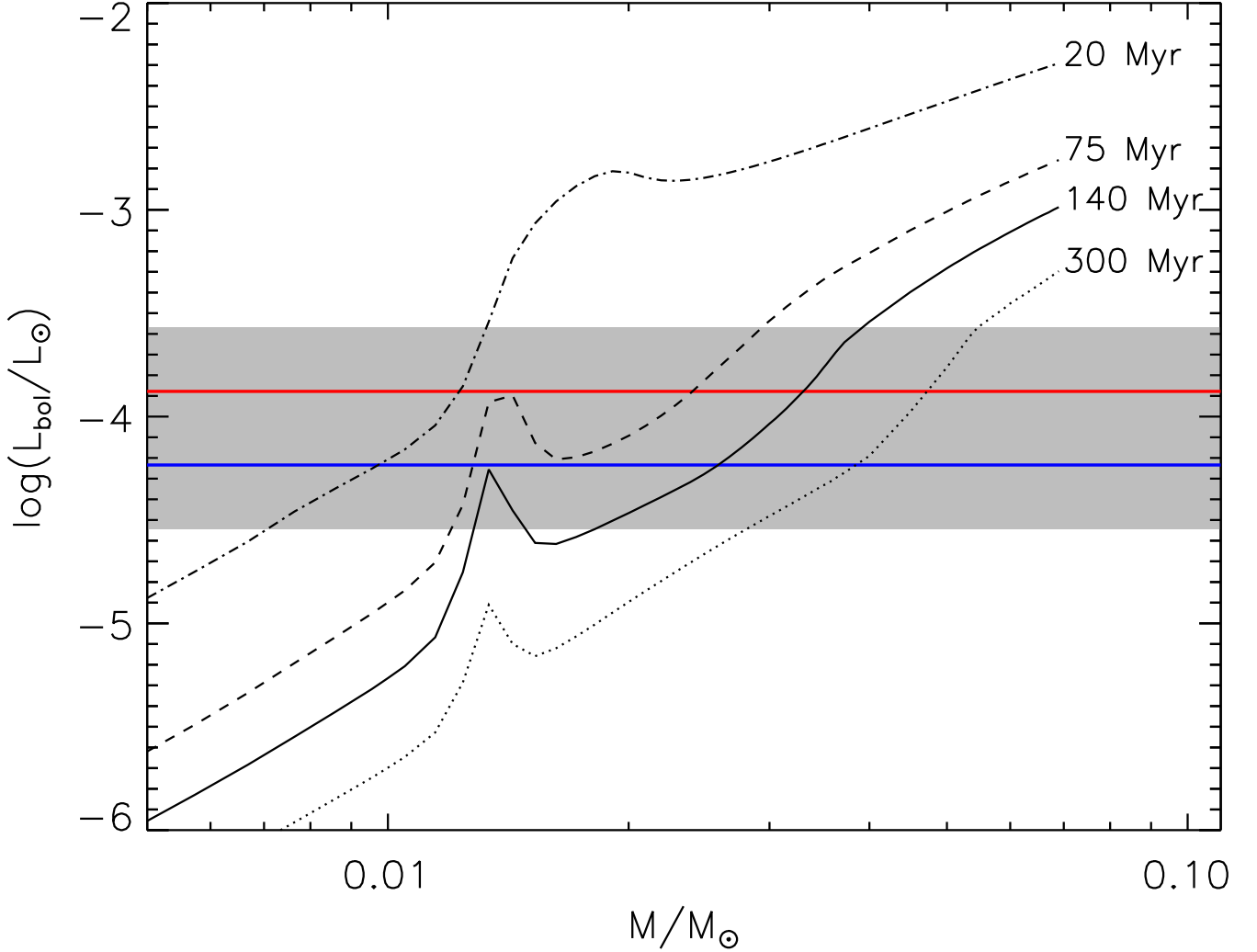


Fig. 8.— Plot of mass vs.  $\log(L_{\text{bol}}/L_{\odot})$  for model isochrones of 20, 75, 140, and 300 Myr (Burrows et al. 1997). The solid horizontal lines show our measured luminosities of SDSS J2249+0044A (red) and B (blue), while the shaded region represents the range of  $1\sigma$  uncertainty. While the absolute luminosities of SDSS J2249+0044A and B are quite uncertain, the relative luminosity (represented by the separation between the red and blue lines;  $0.36 \pm 0.02$  dex) is well determined. The bump in the isochrones at  $\sim 0.013 M_{\odot}$  is due to deuterium burning and means that for the range of possible ages and luminosities of SDSS J2249+0044AB, its mass ratio cannot be robustly determined. In fact, SDSS J2249+0044AB could have a flux reversal due to deuterium burning, where the lower mass object is currently burning deuterium and is thus the more luminous component.

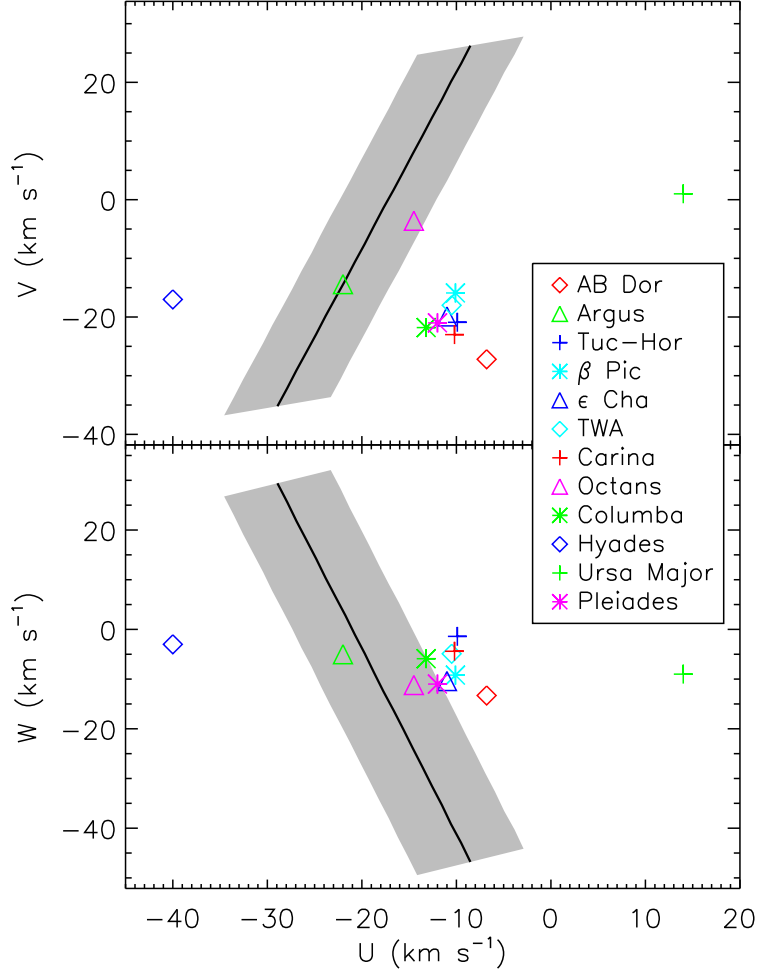


Fig. 9.—  $UVW$  space for SDSS J2249+0044AB and known young moving groups, plotted using a right-handed coordinate system ( $U$  positive toward the Galactic center).  $UVW$  for SDSS J2249+0044AB (solid black line) is calculated from its position, distance, and proper motion for a range of radial velocities ( $-50$  to  $50$   $\text{km s}^{-1}$ ). The gray shaded region shows the region of  $1\sigma$  uncertainty. Note that a broader range of radial velocities would extend the length of the solid black line, but the width of the  $1\sigma$  uncertainty would remain unchanged. The  $UVW$ s of moving groups come from Torres et al. (2008) and Montes et al. (2001). The range of possible space motion for SDSS J2249+0044AB does not overlap most of the known young moving groups with the exception of the Octans and Argus associations, but these associations are in a different part of the sky compared to SDSS J2249+0044AB (Figure 10).

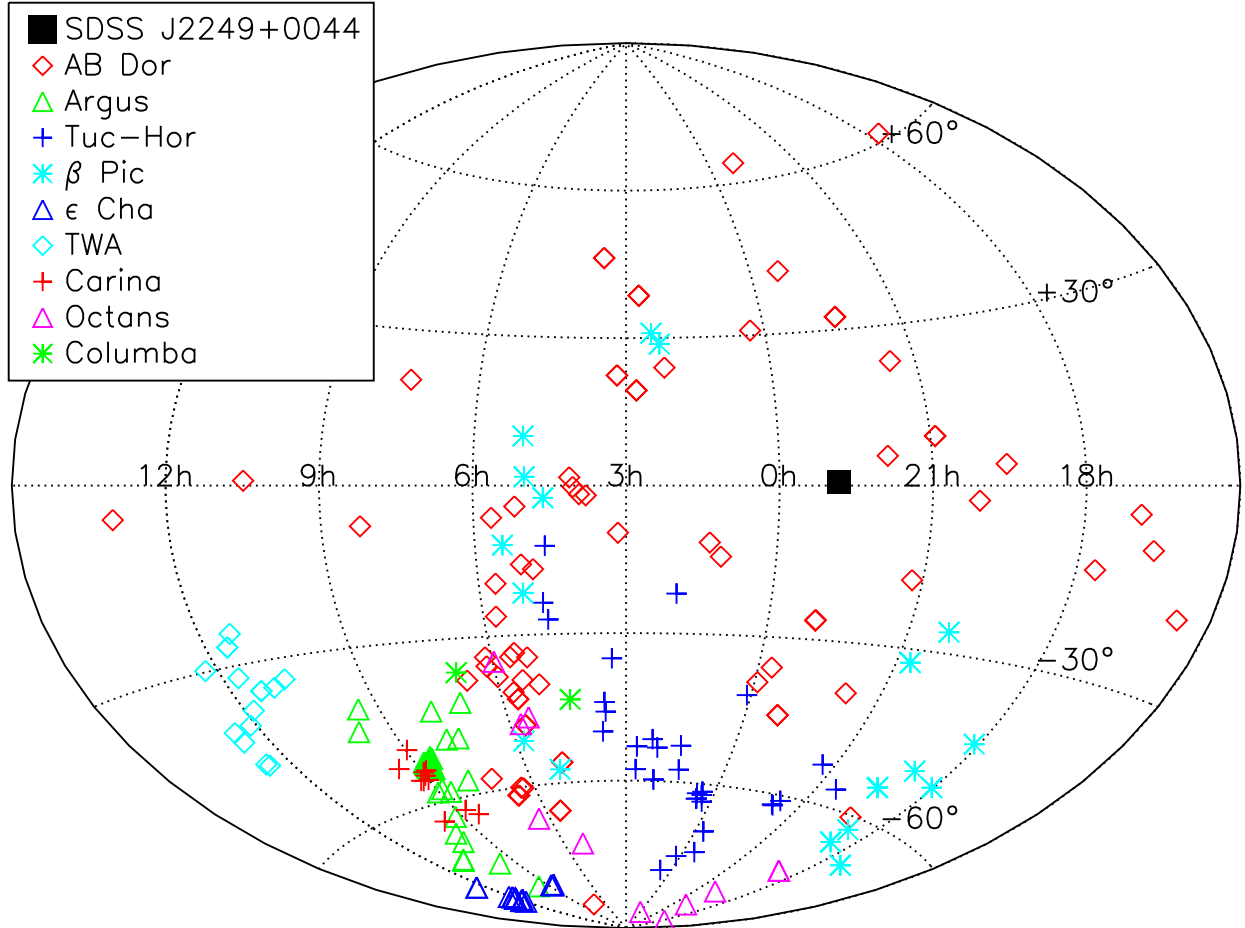


Fig. 10.— Aitoff projection (J2000 equatorial coordinates) showing the positions of SDSS J2249+0044AB and young moving group members from Torres et al. (2008). Argus and Octans, the two young moving groups having space motions that overlap with the possible space motion of SDSS J2249+0044AB, are concentrated deep in the southern hemisphere. Membership of SDSS J2249+0044AB in one of these associations is thus unlikely.